

# Serum-derived extracellular vesicles inhibit osteoclastogenesis in active-phase patients with SAPHO syndrome

Yanpan Gao\*, Yanyu Chen\*, Lun Wang, Chen Li<sup>ID</sup> and Wei Ge<sup>ID</sup>

## Abstract

**Objective:** Synovitis, acne, pustulosis, hyperostosis, and osteitis (SAPHO) syndrome is a rare chronic inflammatory disorder and the underlying pathogenesis is unclear. In this study, 88 SAPHO patients and 118 healthy controls were recruited to investigate the role of serum-derived extracellular vesicles (SEVs) in SAPHO syndrome.

**Methods:** Quantitative proteomics was applied for SEVs proteome identification, and ELISA and Western blotting was performed to verify the results of mass spectrum data. *In vitro* osteoclastogenesis and osteogenesis assay was used to confirm the effects of SEVs on bone metabolism.

**Results:** Tandem mass tagging-based quantitative proteomic analysis of SAPHO SEVs revealed differential expressed proteins involved in bone metabolism. Of these, serum amyloid A-1 (SAA1) and C-reactive protein (CRP) were upregulated. Higher SAA1 levels in SAPHO patients were confirmed by ELISA. In addition, SAA1 levels were positively correlated with CRP, an inflammatory marker related to the condition of patients. *In vitro* cellular studies confirmed that SAPHO SEVs inhibited osteoclastogenesis in patients mainly in the active phase of the disease. Further analysis demonstrated that Nucleolin was upregulated in osteoclasts of active-phase patients under SAPHO SEVs stimulation.

**Conclusion:** In this study, we identified SAA1 as an additional inflammation marker that can potentially assist the diagnosis of SAPHO syndrome, and speculated that Nucleolin is a key regulator of osteoclastogenesis in active-phase patients.

**Keywords:** nucleolin, osteoclast, SAA1, SAPHO syndrome, serum-derived extracellular vesicles

Received: 1 February 2021; revised manuscript accepted: 10 March 2021.

## Introduction

Synovitis, acne, pustulosis, hyperostosis, and osteitis (SAPHO) syndrome is a rare chronic inflammatory disorder involving bone, joints, and skin that was first described in 1987<sup>1</sup> and occurs with an estimated prevalence in Caucasians of <1/10,000.<sup>2</sup> Bone and joint manifestations, including osteitis, synovitis and hyperostosis, are the hallmark of the SAPHO syndrome and affect a variety of regions of the body.<sup>3</sup> It occurs regardless of the presence of active dermatologic findings.<sup>4</sup> Bone and joint damage can induce pain and bone destruction, which cause spinal stiffness, and even vertebral collapse, thereby

affecting the quality of life of patients with SAPHO syndrome.

According to the 2012 Seminars in Arthritis Rheumatism criteria,<sup>4</sup> SAPHO syndrome is classified mainly based on typical clinical manifestations (bone and cutaneous involvement), supplemented by imaging approaches to visualize hyperostosis of the characteristic sites (the anterior chest wall, axial skeleton), and combined with biopsy when necessary. However, no specific laboratory findings can be used to confirm the diagnosis of SAPHO syndrome. Commonly used inflammatory markers, such as C-reactive protein

*Ther Adv Musculoskel Dis*

2021, Vol. 13: 1–17

DOI: 10.1177/  
1759720X211006966

© The Author(s), 2021.  
Article reuse guidelines:  
[sagepub.com/journals-permissions](https://sagepub.com/journals-permissions)

Correspondence to:

**Chen Li**  
Department of Traditional Chinese Medicine, Peking Union Medical College Hospital, Chinese Academy of Medical Sciences and Peking Union Medical College, No. 9 Dong Dan San Tiao, Beijing 100730, China  
[casio1981@163.com](mailto:casio1981@163.com)

**Wei Ge**  
State Key Laboratory of Medical Molecular Biology & Department of Immunology, Institute of Basic Medical Sciences, Chinese Academy of Medical Sciences, No. 5 Dong Dan San Tiao, Beijing, 100005, China  
[wei.ge@chem.ox.ac.uk](mailto:wei.ge@chem.ox.ac.uk)

**Yanpan Gao**  
**Yanyu Chen**  
State Key Laboratory of Medical Molecular Biology & Department of Immunology, Institute of Basic Medical Sciences, Chinese Academy of Medical Sciences, Beijing, China

**Lun Wang**  
Institute of Clinical Medicine, Peking Union Medical College Hospital, Chinese Academy of Medical Sciences & Peking Union Medical College, Beijing, China

\*These authors contribute equally to this work.

(CRP) and erythrocyte sedimentation rate (ESR) are only applied to evaluate the disease status of SAPHO patients.<sup>5</sup> Thus, the diagnosis of SAPHO syndrome is still challenging.

The precise etiopathogenesis of SAPHO syndrome remains unclear. Although microbial infection and genetic mutations have been reported in a few cases of SAPHO syndrome,<sup>6–8</sup> it is generally considered to be an autoinflammatory syndrome.<sup>5</sup> The osteo-articular manifestations in SAPHO patients are closely associated with immune dysregulation, mainly because the skeletal and immune systems share cells and cytokine effectors.<sup>9,10</sup> Immune cells and cytokine effectors have powerful effects on bone metabolism and may be mediated by extracellular vesicles (EVs).<sup>11–13</sup> Previous studies have shown that EVs, mainly exosomes and shed microvesicles, are involved in bone metabolism in both normal physiological and disease states<sup>14,15</sup> likewise in multiple inflammatory diseases.<sup>16</sup> In addition, EVs from monocytes, leukocyte and macrophage exert direct effects on osteoclastogenesis and osteogenesis,<sup>17–19</sup> indicating that EVs function as mediators between the immune system and bone metabolism. As SAPHO syndrome is an inflammatory-mediated disease characterized mainly by systemic osteo-articular damage, we hypothesized that EVs play an important role in bone and joint damage in SAPHO syndrome.

In this study, we explored the role of serum-derived EVs (SEVs) in SAPHO syndrome, focusing mainly on identification of differentially expressed proteins (DEPs) in SAPHO SEVs and the function of SEVs on bone metabolism.

## Materials and methods

### *Patients and healthy controls*

From October 2017 to August 2018, a total of 88 patients with SAPHO syndrome were recruited from the single-center dynamic cohort of SAPHO syndrome in Peking Union Medical College Hospital (PUMCH, Beijing, China).<sup>20</sup> All enrolled patients met the following inclusion criteria: (1) adults ( $\geq 18$  years old); (2) in accordance with the criteria for diagnosis of SAPHO reported by Nguyen *et al.*;<sup>4</sup> (3) anterior chest wall involvement. After enrolment, the blood samples were collected for basic laboratory tests as well as the measurement of inflammatory markers [CRP, ESR] and bone metabolism markers [ $\beta$ -isolated C-terminal peptide ( $\beta$ -CTX), Osteocalcin].

Patient-reported assessments, including Visual Analogue Score for global pain, Bath Ankylosing Spondylitis Disease Activity Index (BASDAI), and Ankylosing Spondylitis Disease Activity Score-CRP (ASDAS-CRP) were also conducted during the same disease episode (within a week) to evaluate the SAPHO syndrome disease activity. According to previous studies, SAPHO syndrome patients with BASDAI score  $\geq 4$  and ASDAS score  $\geq 2.1$ , which indicated currently high disease activity, were defined as the active phase, otherwise patients were deemed to be in the resting phase of the disease. In addition, 118 healthy controls were also recruited from Physical Examination Center of PUMCH. The clinical information of SAPHO patients and healthy controls is shown in Supplemental Table 1.

Of the 88 SAPHO patients, 41 were used for SEVs mass spectrometry analysis and SEVs stimulation, 54 for ELISA, and 36 for peripheral blood mononuclear cells (PBMC) purification. For 118 healthy controls, 56 were used for SEVs MS analysis, 48 for SEVs stimulation, 84 for ELISA, 10 for PBMC purification, and one for human adipose tissue-derived mesenchymal stem cell (hADMSC) purification. The patients and healthy controls used in these experiments are partially overlapped. The enrolment criteria for all patients and healthy controls were the same, with no selection for each experiment. Detailed information is shown in Supplemental Table 1.

The human adipose tissue used in the present study was obtained from donors who underwent liposuction at the Department of Plastic Surgery, PUMCH.

All patients and healthy controls provided written informed consent to participate and the study was approved by the Ethics Committee of PUMCH (No. ZS-994).

### *Isolation of EVs from human serum*

EV isolation by ultracentrifugation was carried out as previously described.<sup>21</sup> Briefly, pooled serum was first centrifuged ( $10,000\times g$  for 30 min at  $4^{\circ}\text{C}$ ) to remove cell debris. The supernatant was filtered ( $0.22\mu\text{m}$  pore size) and then re-ultracentrifuged ( $110,000\times g$  for 90 min at  $4^{\circ}\text{C}$ ) using a Beckman Optima L-100XP Ultracentrifuge. The supernatant was removed, and the pellet containing the SEVs was washed three times with 1 mL phosphate-buffered saline (PBS). The SEVs were then resuspended and dissolved in 8 M urea for tandem

mass tag (TMT)-labeling. The protein concentration was determined using a NanoDrop 2000 spectrophotometer (Thermo Fisher Scientific).

For EV isolation using the Total Exosome Isolation Reagent (from serum) (Life Technologies, Carlsbad, CA, USA), pooled serum samples were diluted with an equal volume of PBS to decrease viscosity, followed by the addition of 0.2 volume of the Total Exosome Isolation Reagent. Samples were vortexed and incubated at 4°C for 30 min. Subsequently, samples were centrifuged (10,000×*g* for 30 min at room temperature) and the pellet containing the SEVs was resuspended in PBS. The SEVs were then lysed with RIPA buffer and the protein content was measured using BCA assay. SEVs isolated by reagent were used for Western blotting, nanoparticle tracking analysis (NTA), and SEVs stimulation *in vitro* osteoclastogenesis and osteogenesis assays.

#### TMT labeling

The detailed TMT labeling procedure is supplied in the supplemental methods. Healthy control SEVs were labeled with TMT-128 and SAPHO SEVs were labeled with TMT-131. For labeling of osteoclasts (OCs) in the response group, the OCs stimulated by healthy SEVs were labeled with TMT-129, and those stimulated by SAPHO SEVs were labeled with TMT-131. In the non-response group, the OCs stimulated by healthy SEVs were labeled with TMT-126 and those stimulated by SAPHO SEVs were labeled with TMT-130.

#### Bioinformatics analysis

The changes in protein expression in SAPHO SEVs were represented as the TMT-131/128 ratio (SAPHO/healthy control). According to the 95% prediction interval,  $\log_2(131/128)$  ratios  $\geq 1.24$  was set as the threshold for upregulated proteins, while  $\log_2(131/128)$  ratios  $\leq -2.17$  were set as the threshold for downregulated proteins. The mass spectrometry proteomics data have been deposited in the ProteomeXchange Consortium *via* the PRIDE partner repository with the dataset identifier PXD012125.

The changes in protein expression in OCs stimulated by SAPHO SEVs were represented by the TMT-131/129 ratio in response group and 130/126 ratio in the non-response group. According to the 95% prediction interval, the  $\log_2(131/129)$  ratio  $\geq 0.20$  was set as the threshold for upregulated proteins in the response group, while the ratio  $\leq -0.22$  was set as the

threshold for downregulated proteins. Similarly, in the non-response group, the  $\log_2(130/126)$  ratio  $\geq 0.21$  was set as the threshold for upregulated proteins, and the ratio  $\leq -0.18$  was set as the threshold for downregulated proteins. The mass spectrometry proteomics data have been deposited in the ProteomeXchange Consortium *via* the PRIDE partner repository with the dataset identifier PXD012218.

Gene ontology (GO) enrichment analyses were carried out using the DAVID online analysis tool (<https://david.ncifcrf.gov/>). Protein–protein interactions were illustrated using Cytoscape software (3.8) based on the STRING app.

#### Cell culture

The details of the methods used for purification of hADMSCs and PBMCs, the induction of osteogenesis from hADMSCs, and osteoclastogenesis from PBMCs are supplied in the supplemental methods.

#### Statistical analysis

The number of OCs was determined by counting Tartrate-Resistant Acid Phosphatase (TRAP) stain-positive cells with more than three nuclei. The area of OCs and mineralized point were measured by Image-J. SPSS 24.0 (IBM Corp., Armonk, NY), and GraphPad Prism (version 7.04; Nashville, TN, USA) software was used for data presentation and statistical analysis. Variables with normal distribution were expressed as mean  $\pm$  standard deviation (SD), while variables with non-normal distribution were expressed as median and interquartile range, unless otherwise indicated. The  $\chi^2$  test was used for comparing the characteristics of patients (sex, BASDAI score, ASDAS score, ESR, CRP,  $\beta$ -CTX and Osteocalcin) in the response and non-response groups. The Mann–Whitney *U*-test analysis was used for non-normally distributed continuous variables (OC area and OC number). For normally distributed continuous variable (age) Student's *t*-test was used. A value of  $p < 0.05$  was considered to indicate statistical significance.

Details of reagents, NTA, high-performance liquid chromatography analysis, liquid chromatography tandem-mass spectrometry (LC-MS/MS) analysis, TMT labeling, protein identification, cell culture, bone resorption assay, TRAP staining, and Alizarin red staining are supplied in the supplemental methods.

## Results

### Project design

A flow chart of the study design is shown in Figure 1. The serum SEVs of 41 SAPHO patients and 56 healthy controls were isolated by ultracentrifugation or using appropriate reagents. The SEVs isolated by ultracentrifugation were used for TMT-based quantitative proteomics and those isolated by reagent were used for Western blotting, NTA and stimulation of osteogenesis and osteoclastogenesis. Expression of the EV markers CD63 and ALIX were verified by Western blotting. The particle diameters and concentration of EVs were evaluated by NTA.

For verification of the mass spectrometry results showing higher SAA1 level in SAPHO SEVs, serum samples from 54 SAPHO patients and 84 healthy controls were analyzed by ELISA.

The function of SEVs in bone metabolism was further investigated in another 36 SAPHO patients and 11 healthy controls. The PBMCs isolated from 36 SAPHO patients and 10 healthy controls were induced to form OCs. The hADMSCs from one healthy control were induced to form osteoblasts (OBs). The effect of SEVs on osteoclastogenesis and osteogenesis were evaluated by TRAP staining and Alizarin red staining, respectively.

While exploring the effect of SEVs on osteoclastogenesis, we found that OC differentiation was inhibited by SAPHO SEVs in 24 SAPHO patients; these patients were classified as the response group. In contrast, no changes under SAPHO and healthy SEV stimulation were observed in the other 12 SAPHO patients; these patients were classified as the non-response group. Statistical analysis and quantitative proteomics were further applied to explain the clinical and molecular mechanisms of the response to SEVs in SAPHO patients.

### Verification of SEVs

The SEVs isolated using reagents were used for Western blotting and NTA analysis. Western blot analysis showed that EV markers CD63 and ALIX were both enriched in the SEV pellet fraction, but not in whole serum and the supernatant fraction (Figure 2a). NTA showed that mean particle diameter of SEVs in the healthy controls and SAPHO patients was 176 nm and 152 nm, respectively (Figure 2b), with no significant difference between these two groups (Figure 2c). In

addition, there was no significant differences in particle concentration of SEVs between healthy controls and SAPHO patients (Figure 2d).

The SEVs purified by ultracentrifugation were used for TMT-based quantitative proteomics. A total of 1620 proteins were identified both in healthy controls and SAPHO patients, of which 803 trusted proteins were identified (score  $\geq 10$ , unique peptide  $\geq 2$ ). The Uniprot Accession numbers of trusted proteins were then mapped to 768 Entrez Gene IDs. Based on the Entrez Gene ID, 692 of 768 proteins (90%) overlapped with the ExoCarta database (Figure 2e, <http://www.exocarta.org>, release date: 29 July 2015).

GO analysis showed that the total proteins identified in SEVs were mainly enriched in immune regulation-related process, such as complement activation, Fc $\gamma$  receptor signaling pathway, and proteolysis (Figure 2f), and located in the extracellular matrix, extracellular region, extracellular space, and exosome (Figure 2g). The molecular functions of these proteins were antigen binding, heparin binding, and cadherin binding involved in cell–cell adhesion (Figure 2h). These data indicated that the purification of EVs from serum was successful.

### Characteristics of DEPs in SAPHO SEVs

Based on the criteria list in the Materials and Methods section, 49 DEPs were filtered in SAPHO SEVs with 10 proteins upregulated and 39 downregulated (Supplemental Table S2). GO analysis showed that the downregulated proteins were enriched in the following biological processes: platelet degranulation, signal peptide processing, peptidyl-glutamic acid carboxylation, and extracellular matrix organization (Figure 3a). Apart from the extracellular space, extracellular region, and extracellular exosome, the downregulated proteins also located in EVs generating cell organelles, such as endoplasmic reticulum lumen, platelet alpha granule lumen, and Golgi lumen (Figure 3a). In addition, the enriched molecular functions were bone metabolism related, such as endopeptidase inhibitor activity, calcium ion binding, collagen binding, and heparin binding (Figure 3a). The upregulated proteins were not significantly enriched in any GO items, but nonetheless, CRP and SAA1, two acute-phase proteins, are highly related to immune response and inflammation. The protein–protein interaction analysis based on STRING database showed close interconnection between the DEPs (Figure 3b).

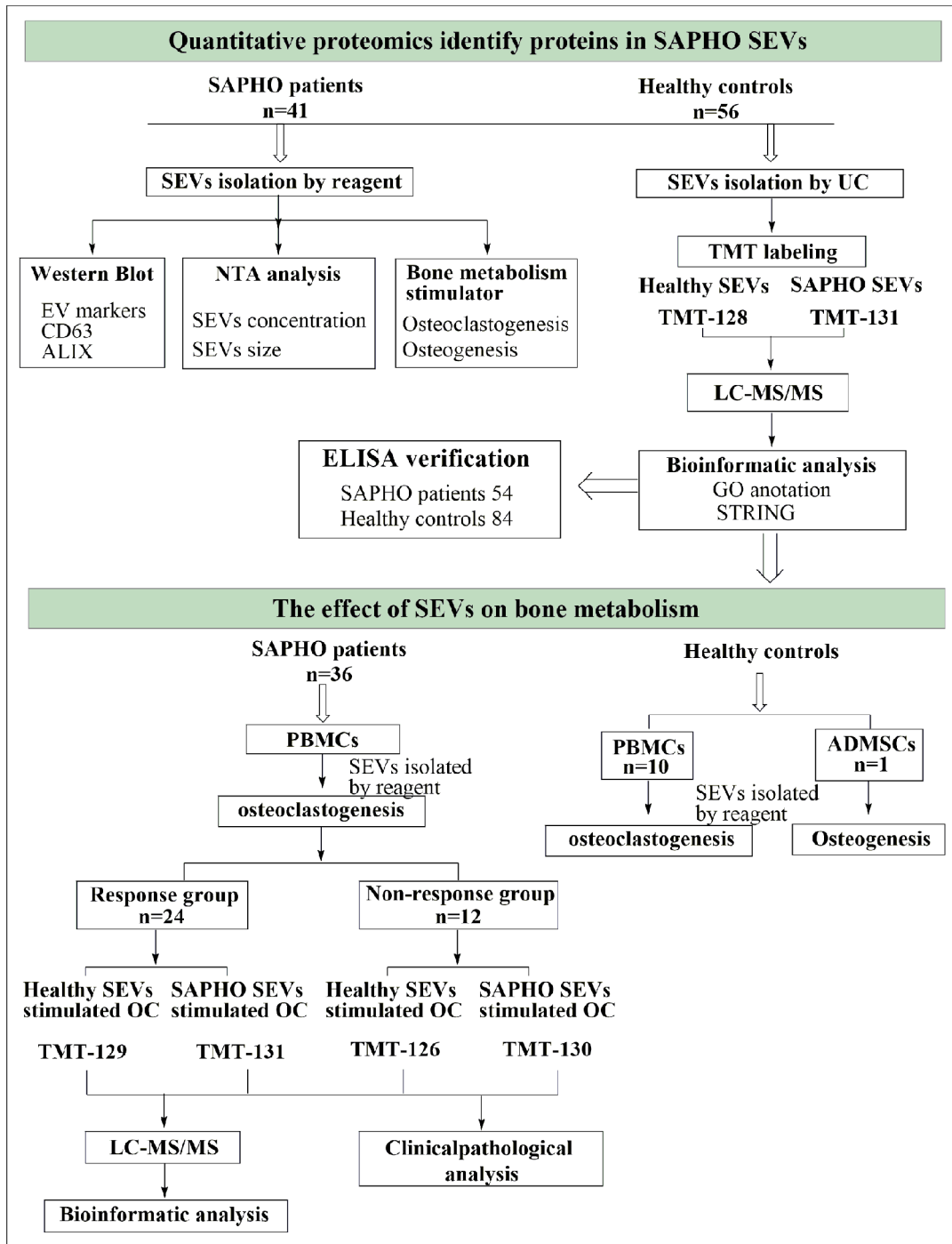


**Figure 1.** The workflow of the project.

SEVs, serum-derived extracellular vesicles; EV, extracellular vesicles; NTA, nanoparticle tracking analysis; UC, ultracentrifugation; TMT, tandem mass tag; LC-MS/MS, liquid chromatography tandem-mass spectrometry; GO, gene ontology; STRING, protein-protein interaction networks analysis by STRING (version 11.0); PBMCs, peripheral blood mononuclear cells; ADMSCs, adipose tissue-derived mesenchymal stem cells; OC, osteoclast.

### *SAA1 is highly expressed in SAPHO patients*

CRP is a laboratory inflammatory indicator associated with high levels of disease activity in SAPHO patients.<sup>19</sup> However, the relationship

between SAA1 and SAPHO remains unclear. To investigate this relationship, we analyzed the levels of SAA1 in 54 SAPHO patients and 84 healthy controls by ELISA. Compared with the healthy

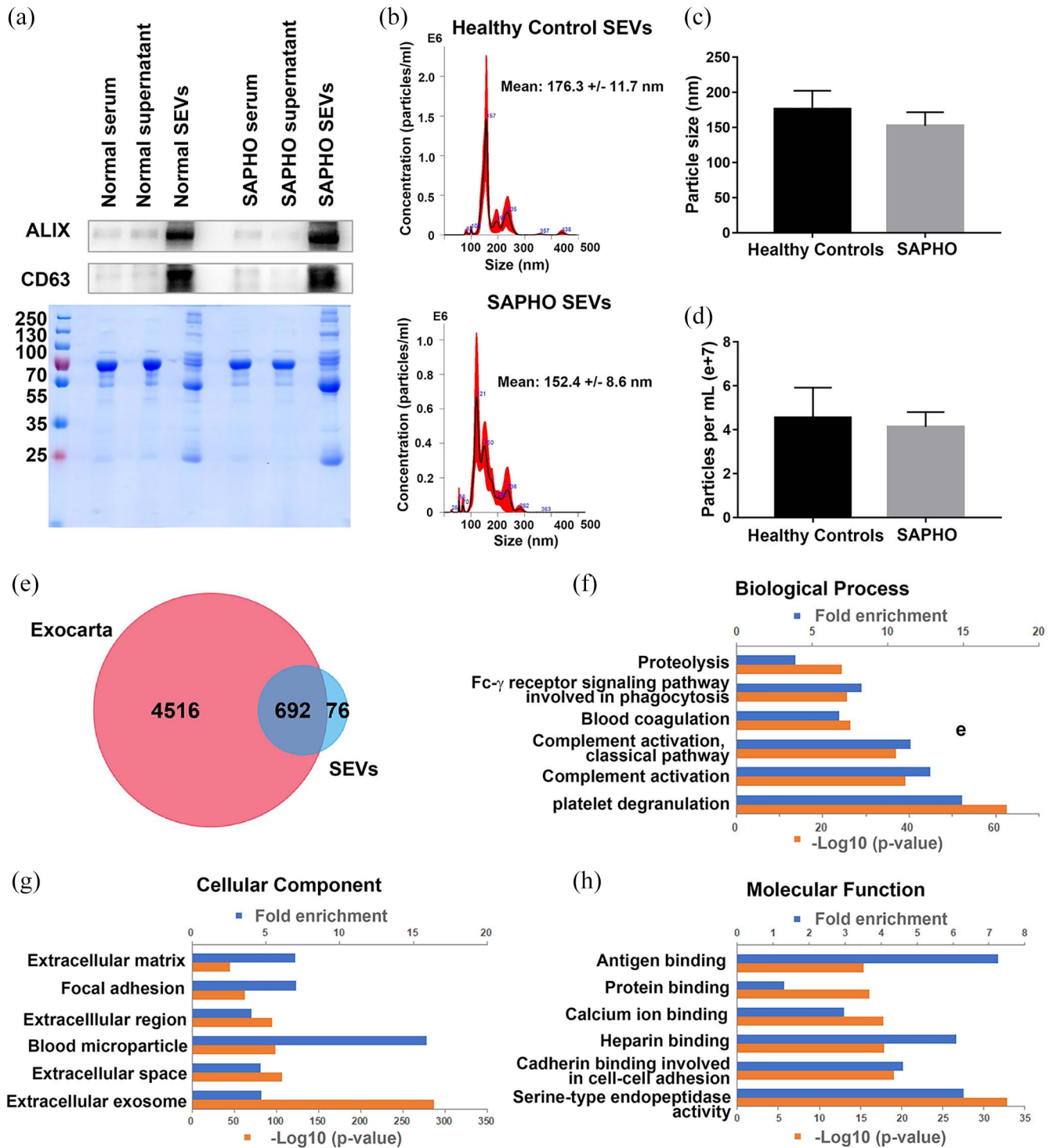


**Figure 2.** Serum-derived extracellular vesicle (SEV) purification and identification. (a) Purified SEVs were verified by Western blot detection of EV markers ALIX and CD63. Equal amounts of proteins from each sample were loaded. The Coomassie Blue staining of the total proteins separated by SDS-PAGE is shown. (b) Nanoparticle tracking analysis (NTA) analysis of SEVs of SAPHO patients and healthy controls. (c) The particle size of two types of SEVs. (d) The particle concentration of two types of SEVs. (e) The overlapped proteins between identified SEVs proteins and the ExoCarta database. (f–h) Gene ontology annotation of SEVs proteins identified by mass spectrometry based on biological process (f), cellular component (g), and molecular function (h).

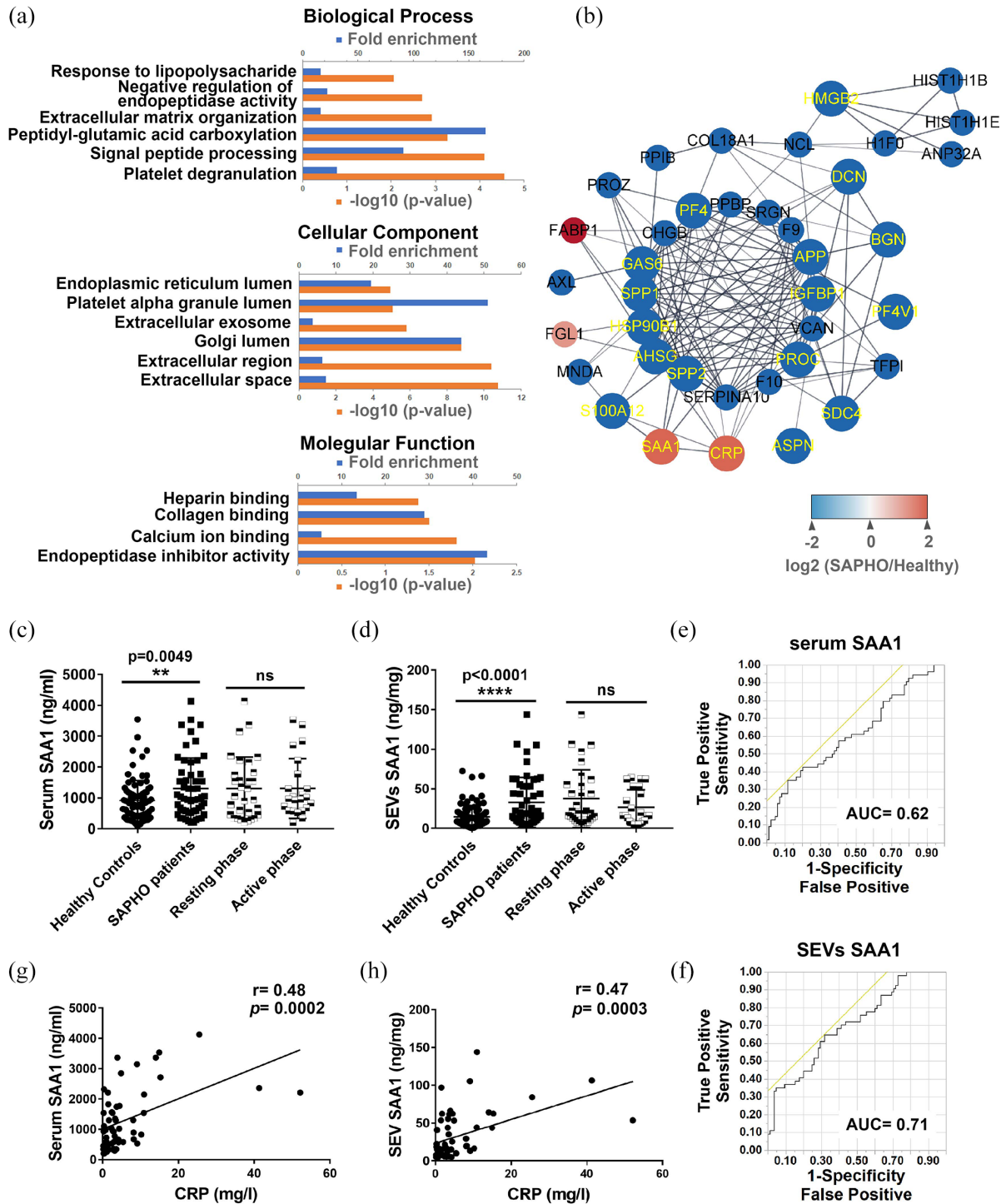


**Figure 3.** Biological analysis of DEPs in SAPHO SEVs. (a) Gene ontology annotation of the DEPs identified by mass spectrometry in SAPHO SEVs based on biological process, cellular component, and molecular function. (b) The protein-protein interaction network of DEPs in SAPHO SEVs, constructed using the STRING online tool. Red represents upregulation and blue represents downregulation. The proteins involved in bone metabolism are shown in yellow text. (c) Serum SAA1 levels in healthy controls and SAPHO patients detected by ELISA. (d) SEVs SAA1 levels of healthy controls and SAPHO patients detected by ELISA. In (c) and (d), the patients were further separated into resting and active-phase groups and the SAA1 levels was compared. (e, f) ROC curve analysis of the SAA1 in serum (e) and SEVs (f) for SAPHO diagnosis. (g, h) Pearson correlation analysis of CRP levels with serum (g) and SEVs SAA1 levels (h). Data represent the mean  $\pm$  standard deviation. \*\* $p < 0.01$ , \*\*\*\* $p < 0.0001$ , two-tailed unpaired  $t$ -test. SAA1, Serum amyloid A-1; SEVs, serum-derived extracellular vesicles; AUC, area under curve; CRP, C-reactive protein.

controls, the SAA1 level of SAPHO patients was elevated both in serum and SEVs (Figure 3c and 3d). However, there was no significant difference between the resting and active phases of the disease. Furthermore, receiver operating characteristic (ROC) curve analysis showed that SAA1 could be used to distinguish SAPHO patients from healthy controls with moderate accuracy, with an area under the curve (AUC) of 0.62 for serum SAA1 and AUC 0.71 for SEVs SAA1 (Figure 3e and 3f). The best cut-off value for serum SAA1 was identified as 1539.47 ng/ml, with a specificity of 0.88 and a sensitivity of 0.35. For SEVs, the best cut-off value was identified as 15.12 ng/mg, with a specificity of 0.68 and a sensitivity of 0.65. Pearson correlation analysis showed that SAA1 was positively correlated with serum CRP, both in serum ( $r=0.48$ ,  $p=0.0002$ , Figure 3g) and SEVs ( $r=0.47$ ,  $p=0.0003$ , Figure 3h). These results implicated that SAA1, as an additional inflammation marker, may potentially assist SAPHO diagnosis.

#### *SAPHO SEVs inhibit osteoclastogenesis in SAPHO patients in the active phase of the disease*

Of the 49 DEPs, 18 proteins (37%) were identified as bone metabolism regulators, which were labeled with yellow in STRING network (Figure 3d). The details of protein function in bone metabolism are shown in Table 1. This result indicated that SEVs play roles in the abnormal bone metabolism associated with SAPHO.

To investigate the influence of SEVs on osteoclastogenesis in SAPHO patients, PBMCs were purified and OC differentiation was induced. In 24 (2/3) SAPHO patients, osteoclastogenesis was significantly inhibited by SAPHO SEVs. TRAP staining revealed significantly fewer and smaller OCs under SAPHO SEVs stimulation than that under healthy SEVs stimulation (Figure 4a). In the other 12 cases, however, there were no significant differences between OCs stimulated by SEVs derived from SAPHO patients and healthy controls (Figure 4b). Detailed statistical results of OC area and number were shown in Figure 4c. The patients with inhibited OCs by SAPHO SEVs were classified as the response group, and those with no changes in OCs were classified as the non-response group. Representative TRAP staining images of OCs of all 36 SAPHO patients are shown in Supplemental Figure S1.

To investigate the potential correlation of clinical factors and patients' responses, the clinical features of SAPHO patients in the response and non-response group were compared and assessed (Table 2). Chi-square test showed that the patients' response was associated with BASDAI score ( $|r_s|=0.378$ ,  $p=0.023$ ), ASDAS score ( $|r_s|=0.359$ ,  $p=0.031$ ) and CRP level ( $|r_s|=0.347$ ,  $p=0.037$ ). According to both the BASDAI score (8/8) or ASDAS score (13/15), it can be seen that almost all the active-phase patients were within the response group. However, for the resting-phase patients, there was no significant difference of patients' number in the response and the non-response groups, with approximately even distribution. This indicates that SAPHO patients in the active phase are more susceptible to the effects of SAPHO SEVs on osteoclastogenesis than those in the resting phase. In addition, the patients' response was not correlated with demographic characteristics (such as sex and age) and bone metabolism markers (such as Osteocalcin and  $\beta$ -CTX).

#### *SAPHO SEVs have no influence on osteoclastogenesis and osteogenesis in healthy people*

The function of SEVs on bone metabolism in healthy individuals was evaluated in 11 healthy controls. TRAP staining showed that both healthy and SAPHO SEVs promote the OC differentiation, but no significant difference was observed between the effects of the two types of SEVs (Figure 4d–f). Representative TRAP staining images of 10 healthy controls are shown in Supplemental Figure S2.

To evaluate the effect of SEVs on osteogenesis in healthy individuals, *in vitro* osteogenesis assay was performed. Human ADMSCs from healthy controls were incubated with  $\beta$ -GP, L-AA, and dexamethasone to induce OB formation in the presence or absence of SEVs. After 24 days, calcium nodules appeared and were stained with Alizarin Red S. The result showed that there were no significant differences in the calcium nodes formed under stimulation with PBS, SEVs derived from SAPHO patients, or SEVs derived from healthy controls (Figure 4(g) and 4h). These results suggested that SAPHO SEVs did not disturb the osteoclastogenesis and osteogenesis processes in healthy individuals.



**Table 1.** Bone metabolism related DEPs.

UniProt accession	Gene name	SAPHO/normal	Effect on bone metabolism	Reference
P0DJ18	SAA1	1.92	Inhibit osteoclast differentiation	Kim <i>et al.</i> <sup>22</sup> and Oh <i>et al.</i> <sup>23</sup>
P02741	CRP	1.92	Inhibit osteoclast differentiation	Kim <i>et al.</i> <sup>24</sup>
P80511	S100A12	-2.20	Enhance osteoclast differentiation	Nishida <i>et al.</i> <sup>25</sup>
P08833	IGFBP1	-2.24	Enhance osteoclastogenesis and enhance bone resorption	Wang <i>et al.</i> <sup>26</sup>
P05067	APP	-2.58	Enhance osteoclast function	Li <i>et al.</i> <sup>27</sup>
P21810	BGN	-2.67	Enhance osteoblast differentiation. Inhibit osteoclast differentiation.	Bi <i>et al.</i> <sup>28</sup> and Parisuthiman <i>et al.</i> <sup>29</sup>
Q9BXN1	ASPN	-2.81	Inhibit bone formation	Ikegawa <sup>30</sup> and Ueda <i>et al.</i> <sup>31</sup>
Q14393	GAS6	-2.95	Enhance osteoclastogenesis. <i>Via</i> binding to Tyro 3 receptor tyrosine kinase.	Nakamura <i>et al.</i> <sup>32</sup>
P26583	HMGB2	-3.04	Enhance osteoclastogenesis	Yamoah <i>et al.</i> <sup>33</sup>
P31431	SDC4	-3.06	Inhibit osteoclast differentiation. <i>Via</i> binding to M-csf.	Kim <i>et al.</i> <sup>34</sup>
P07585	DCN	-3.12	Inhibit osteoclast differentiation	Li <i>et al.</i> <sup>35</sup>
P10720	PF4V1	-3.21	Inhibit osteoclast resorption	Horton <i>et al.</i> <sup>36</sup>
P10451	SPP1	-3.24	Inhibit osteoclast resorption. <i>Via</i> reduce CD44 expression.	Chellaiah <i>et al.</i> <sup>37</sup> and Reinholt <i>et al.</i> <sup>38</sup>
Q13103	SPP2	-3.24	Inhibit new bone formation	Tian <i>et al.</i> <sup>39</sup>
P04070	PROC	-3.66	Inhibit osteoclast fusion. <i>Via</i> binding to EPCR, PAR-1, S1P receptor, and ApoER2.	Yoshida <i>et al.</i> <sup>40</sup>
P02765	AHSG	-3.86	Regulate osteoblast differentiation. <i>Via</i> TGF-beta/BMP signaling.	Szweras <i>et al.</i> <sup>41</sup>
P02776	PF4	-4.47	Inhibit osteoclast resorption	Horton <i>et al.</i> <sup>36</sup>

*Antigen presentation-associated proteins are downregulated in OCs of patients in response group under SAPHO SEVs stimulation*

To clarify the molecular mechanisms of the response of SAPHO patients to SEVs, we analyzed the proteomic differences between OCs from SAPHO patients in the response and non-response groups (Figure 1). The identified total and DEPs are shown in Supplemental Table 3. The ratios of TMT-131/129 and TMT-130/126 were determined as a representation of the changes induced by SAPHO SEVs in response group and non-response group, respectively. The DEPs in the response group and the non-responsive group were screened out based on the 95% prediction interval.

Protein expression heatmaps showed dramatic differences between the DEPs in the response and non-response group (Figure 5a). The overlaps of the upregulated and downregulated proteins between the two groups were less than 18% and 34%, respectively (Figure 5b and 5c). The protein-protein interaction network of DEPs in the response group showed that the downregulated proteins were enriched in the antigen processing and presentation process, including MHC class I protein (HLA-A, HLA-C, LILRB4, TAPBP), MHC class II proteins (HLA-DRA, HLA-DRB1, HLA-DRB5, HLA-DPA1, CD74), and the Fcγ receptor family proteins (FCGR1A and FCGR3A) (Figure 5d).

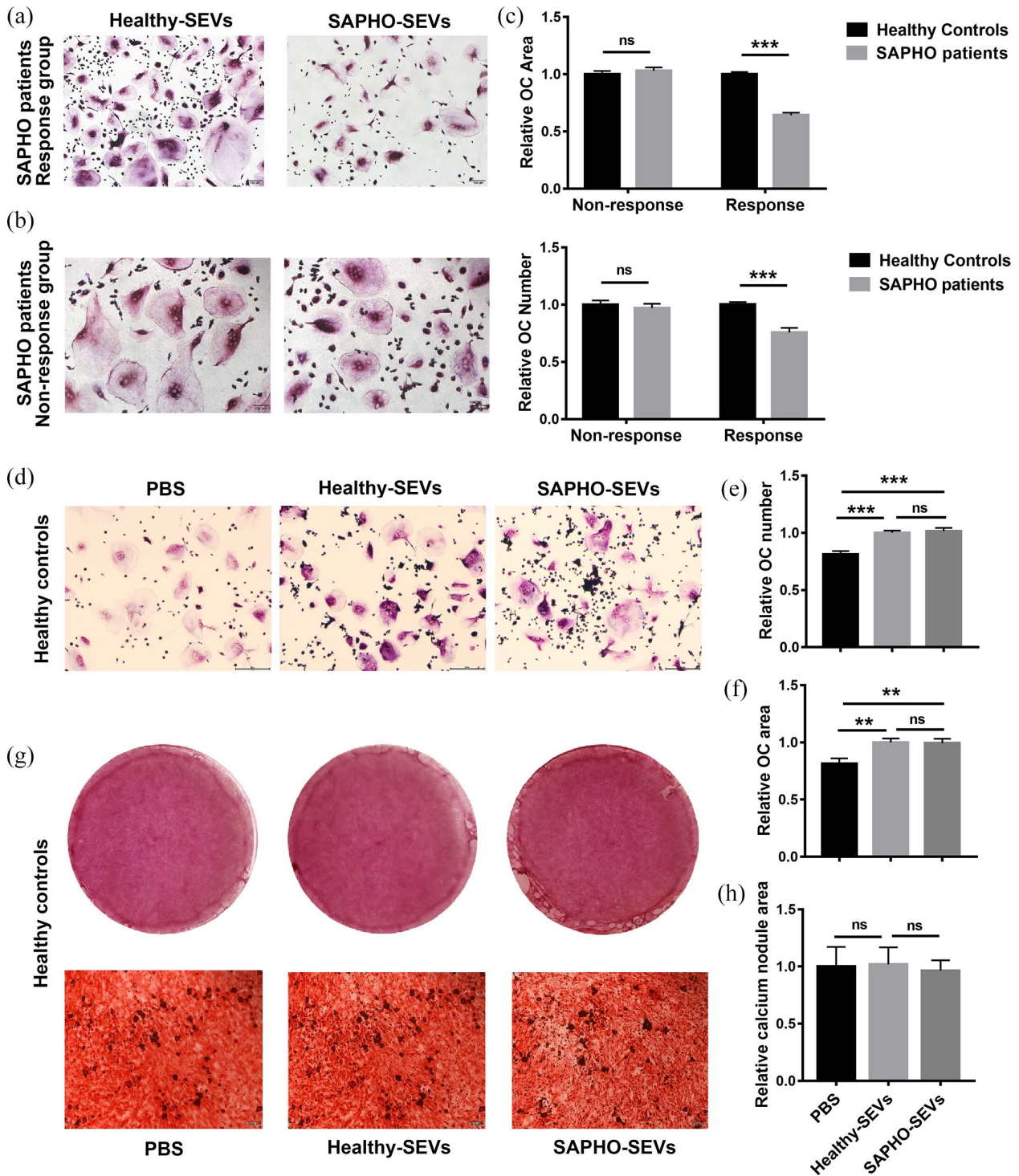


**Figure 4.** SAPHO SEVs inhibit osteoclastogenesis in SAPHO patients in the active phase of the disease. (a, b) Representative TRAP staining images of OCs in patients in the response group (a) and the non-response group (b) under SEVs stimulation. The TRAP staining images of each patient are shown in Supplemental Figure S1. (c) OC number and area calculation and comparison. The average number or area of OCs in each patient stimulated by healthy SEVs was normalized to 1. (d) Representative TRAP staining images of OCs in healthy controls under SEVs or PBS stimulation. (e, f) OC number (e) and area (f) calculation and comparison. The average number or area of OCs in each healthy control stimulated by healthy SEVs was normalized to 1. (g) Alizarin red staining images of calcium node in osteoblasts differentiated from human ADMSCs under SEVs or PBS stimulation. (h) Calcium node area calculation and comparison of osteoblasts differentiated from ADMSCs under SEVs or PBS stimulation. Data represent the mean  $\pm$  standard deviation. \*\*\* $p < 0.001$ , two-tailed unpaired  $t$ -test. SEVs, serum-derived extracellular vesicles; OC, osteoclast.

**Table 2.** Relationship between patient response and clinical features.

Variables	SAPHO patients		$ r_s $	<i>p</i> -Value
	Non-response ( <i>n</i> = 12)	Response ( <i>n</i> = 24)		
Relative OC area	1.02 (0.97, 1.07)	0.71 (0.53, 8.82)		<b>&lt;0.001*</b>
Relative OC number	0.97 (0.91, 1.03)	0.66 (0.49, 0.85)		<b>0.005*</b>
Sex				0.806
Male	4 (33.3%)	9 (37.5%)		
Female	8 (66.7%)	15 (62.5%)		
Ages (years)	40.08 ± 13.69	42.04 ± 14.96		0.706
BASDAI	2.05 (0.15, 2.80)	2.63 (1.50, 6.53)	0.378	<b>0.023*</b>
Low disease activity (<4)	12	16		
High disease activity (≥4)	0	8		
ASDAS (CRP)	1.41 (1.02, 1.68)	2.23 (1.07, 3.64)	0.359	<b>0.031*</b>
Moderate disease activity or inactive disease (≤2.1)	10	11		
High disease activity (>2.1)	2	13		
ESR (mm/h)	10 (7, 17.5)	11.5 (5.25, 24.5)		0.629
≤15	4	14		
>15	8	10		
CRP (mg/L)	2.07 (0.93, 5.25)	3.06 (0.67, 11.59)	0.347	<b>0.037*</b>
≤8	12	17		
>8	0	7		
β-CTX	0.83 (0.60, 2.66)	1.33 (0.50, 5.75)		0.571
Osteocalcin	2.59 (0.64, 4.50)	1.81 (1.29, 2.92)		0.678

\*Statistically significant (*p* < 0.05).  
 OC, osteoclast; ESR, erythrocyte sedimentation rate CRP, C-reaction protein; β-CTX, β-isolated C-terminal peptide.  
 The bold indicates significant difference.

### *Nucleolin is a core protein involved in osteoclastogenesis in response group patients under SAPHO SEVs stimulation*

The proteins that were upregulated in the OCs from the patients in the response group following stimulation by SAPHO SEVs were enriched in cellular processes including chromatin organization, pre-mRNA processing, mRNA pre-treatment, ribosome organization and mitochondria. These proteins were linked by Nucleolin (NCL) (Figure 5e). Western blot analysis verified higher NCL level in response group OCs stimulated by SAPHO SEVs. In contrast, there

was no difference of NCL level between the OCs stimulated by SAPHO SEVs and healthy SEVs in the non-response group (Figure 5f).

## Discussion

### *SAA1 as an inflammation marker may potentially assist SAPHO syndrome diagnosis*

SAPHO syndrome is a chronic inflammatory disease involving bone, joints, and skin, with unclear etiology and pathogenesis. The diagnosis of SAPHO

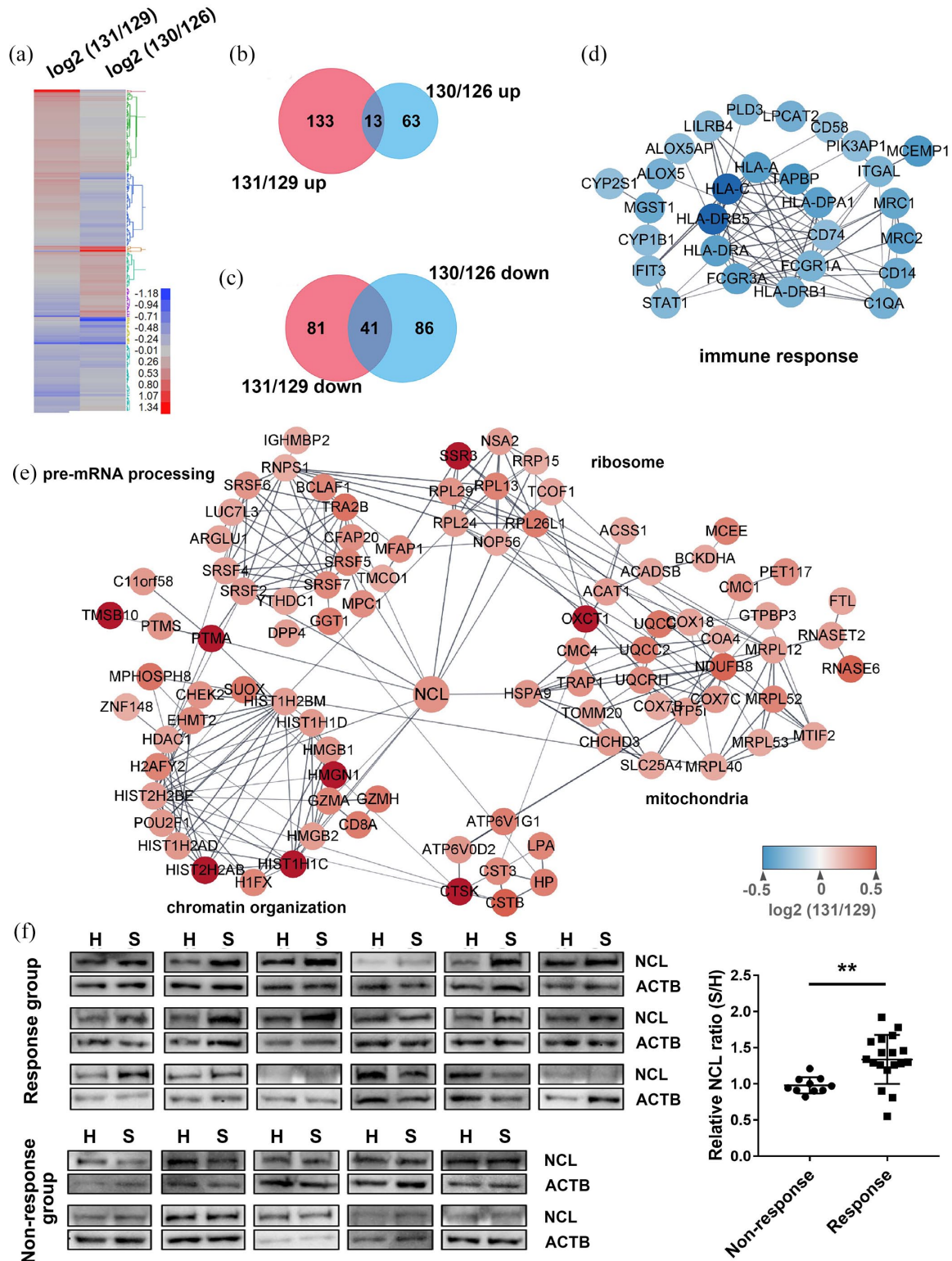


**Figure 5.** Bioinformatic analysis of DEPs in OCs in the response group patients. (a) Heatmap of DEPs in OCs from the response (131/129) and non-response (130/126) group under SAPHO SEVs stimulation. (b, c) Venn diagram of upregulated proteins (b) and downregulated proteins (c) in the response (131/129) and non-response (130/126) group. (d, e) Protein-protein interaction network of downregulated proteins (d) and upregulated proteins (e) in OCs of response group patients under SAPHO SEVs stimulation. (f) Western Blot verification of NCL upregulation in OCs of the response group patients under SAPHO SEVs stimulation. No changes in NCL expression were induced by SAPHO SEVs in the non-response group. Grayscale analysis results are displayed in dot plots. Data represent the mean  $\pm$  standard deviation. **\*\*** $p < 0.01$ , two-tailed unpaired  $t$ -test. H, healthy; S, SAPHO; NCL, nucleolin; ACTB, beta actin.

syndrome is based mainly on the clinical manifestations and radiological or magnetic resonance imaging. Due to the variety of clinical manifestations and sharing features with other established disease categories, the accurate diagnosis of SAPHO syndrome remains challenging. At present, there are no specific diagnostic laboratory tests of SAPHO. Although laboratory tests of non-specific inflammatory markers such as CRP and ESR are commonly used to evaluate the condition of patients, no consistent correlation with SAPHO has been identified.<sup>20,42–44</sup>

Higher circulating concentrations of the acute-phase protein SAA1 are associated with inflammatory conditions,<sup>45,46</sup> such as rheumatoid arthritis (RA) and ankylosing spondylitis (AS).<sup>47–49</sup> In the current study, using 54 SAPHO patients and 84 healthy controls, we found that SAA1 levels were increased in SAPHO patients, and were correlated with CRP levels. ROC curves analysis indicated that SAA1 could distinguish SAPHO patients from healthy controls with moderate accuracy. In addition, to evaluate whether SAA1 could also distinguish SAPHO from other inflammation disease, 22 RA and 29 AS patients were recruited and their SEVs' SAA1 level was also detected. We found that SAA1 level was increased in SAPHO, RA and AS patients compared with healthy controls. However, no significant difference was seen among SAPHO, RA and AS patients, although the level of SEVs' SAA1 in SAPHO is slightly higher than that in RA and AS patients, especially in AS patients (Supplemental Figure S3). Due to the limitation of the number of patients and the type of disease, a definite conclusion could not be drawn. Thus, to determine whether SAA1 could be an additional inflammation marker assist SAPHO diagnosis, a larger sample size and more disease types are required.

Wekell *et al.*<sup>50</sup> reported that SAA1 appears to be a more sensitive inflammatory marker than CRP when monitoring the improvement (the resting) and relapses (the active) phase in SAPHO syndrome. However, our small-scale study showed that there were no significant differences in SAA1 levels between SAPHO patients in the active and resting phase of the disease, which is not consistent with the finding of Wekell *et al.*<sup>50</sup> It can be speculated that this discrepancy is due to differences in the focus of these two studies, with our study comparing SAA1 levels between different patients in the resting and active phases, whereas Wekell and colleagues investigated the dynamic changes of SAA1 in the same patients during disease

progression. This difference may also be related to the wide difference in sample sizes in these two studies, with only two patients recruited into the study conducted by Wekell *et al.* Thus, whether SAA1 could be used as a monitoring marker for disease activity still needs to be studied.

#### *SAPHO SEVs inhibit osteoclastogenesis in patients in the active phase of the disease*

SAPHO syndrome is a stable entity, with a good long-term prognosis.<sup>42,43</sup> The osteoarticular manifestations in patients with SAPHO syndrome show little progression over more than 5 years. A few patients achieve disease-free status after a limited course lasting 3–6 months. And most patients have a chronic course characterized by fluctuating intermittent periods of exacerbation and short-term improvement. During the active phase (exacerbation period), osteolysis occurs in the sternoclavicular joint, causing pain. After a period of time, the osteolysis disappears and the pain is relieved for unknown reasons, and the patient enters the resting phase (improvement period). This relapsing–remitting course and good prognosis suggests that the patients may have self-relief ability. At present, the mechanism regulating the transition from active to resting phase is still unclear. Our results show that SAPHO SEVs specifically inhibit osteogenesis in patients in the active phase of the disease, suggesting that some unknown factors in SEVs may induce the transition from the active to the resting phase.

#### *NCL plays roles in osteoclastogenesis in active phase: Patients under SEVs stimulation*

NCL, which is the major nucleolar protein in eukaryotic cells, is involved in chromatin decondensation and ribosome synthesis and maturation.<sup>51–53</sup> Our proteomic data analysis showed that NCL is a core protein connecting proteins in pre-RNA processing, ribosome, and chromatin organization-related proteins, which is consistent with previous reports.<sup>52,54</sup> Proteins in the mitochondria, a key cellular organelle in OC differentiation,<sup>55,56</sup> were also linked with NCL by HSPA9. Furthermore, in our previous study, we observed high levels of NCL protein in patients with osteopenia and osteoporosis, indicating NCL promotes osteoclastogenesis.<sup>57</sup> These results implicate NCL as a novel regulator of OC differentiation, possibly through regulation of chromatin organization, pre-mRNA processing, and mitochondria. However, further studies are required to clarify the exact role of NCL in OC differentiation.

### *SEVs negatively regulate immune responses in active-phase SAPHO patients*

EVs are involved in numerous physiological processes, and vesicles from both immune and non-immune cells have important roles in immune regulation.<sup>58</sup> Immunized blood-borne EVs have been shown to reduce an active immune response to a specific antigen.<sup>59</sup> It has been hypothesized that SEVs suppress body responses to peripheral self-antigens and to commonly encountered foreign antigens to inhibit chronic inflammation and autoimmunity.<sup>58</sup>

SAPHO is generally considered as an autoinflammatory syndrome, with elevated pro-inflammatory cytokines (IL-1, IL-8, IL-17, and IL-18) and Th17 cells,<sup>5,60</sup> implying that patients are under a highly inflammatory condition. Indeed, SAPHO patients are mostly suffering from long-term chronic inflammation. Antigen-presenting cells express higher levels of MHC class II proteins under inflammatory condition, thereby enhancing self-antigen presentation,<sup>61</sup> suggesting that SAPHO patients are likely to have autoimmune reactions. However, current reports suggest that there is no significant increase in self-antigen content in SAPHO patients.<sup>62</sup> OCs are derived from monocytes/macrophages and inherit the characteristics of monocytes as antigen-presenting cells, including the capacity to engulf pathogens and present antigens to T cells *via* MHC family proteins.<sup>63,64</sup> In this study, SAPHO SEVs reduced the OC expression of proteins in MHC and FCGR families, which play important roles in the antigen presentation process. It is reasonable to speculate that SEVs weaken the self-antigen presentation ability, thereby ameliorating the responses to self-antigens in SAPHO patients. In addition, a previous study showed that loss of MHC class II proteins does not alter osteoclastogenesis and osteogenesis;<sup>65</sup> therefore, we speculate that the SAPHO SEVs regulate the antigen presentation process and osteoclastogenesis in parallel, rather than being a causal relationship. The effects of SEVs on antigen presentation may also promote the transition of SAPHO patients from the active to the resting phase of the disease. Further investigation of the role of SAPHO SEVs in antigen presentation may provide a greater understanding of the pathogenesis of SAPHO syndrome and potential therapeutic strategies.

### *Limitations*

Since SAPHO is a rare disease, the sample size of patients included in this study is limited. SAA1 is

considered as a non-specific inflammatory marker, which is elevated in a variety of inflammatory diseases, like RA and AS. A diagnostic marker specific for SAPHO should not only be able to distinguish SAPHO from healthy status, but also from other inflammation-related diseases that have clinical manifestations similar to SAPHO, including RA and AS. Therefore, SEVs' SAA1 levels were also detected in patients with RA and AS. We obtained some preliminary results. However, due to the limitation of the number of patients and the type of disease, a definite conclusion could not be drawn. Thus, further studies with larger sample size and more disease types are required to determine whether SAA1 as an inflammation marker could assist the diagnosis of SAPHO syndrome.

### **Conclusion**

This study speculates that SAA1, as an additional inflammation marker, may assist SAPHO syndrome diagnosis. This study also shows that the SAPHO SEVs inhibit osteoclastogenesis in active-phase patients, and demonstrates the role of NCL as a core regulator in this process. However, further studies are required to evaluate the diagnostic performance of SAA1 and fully elucidate the specific mechanism by which SEVs affect osteoclastogenesis.

### **Conflict of interest statement**

The authors declare that there is no conflict of interest.

### **Ethics approval**


The experiments were conducted with full compliance with local, national, ethical, and regulatory principles and local licensing regulations. This study was approved by the Ethics Committee of PUMCH (No. ZS-994).


### **Funding**

The authors disclosed receipt of the following financial support for the research, authorship, and/or publication of this article: Yanpan Gao was supported by the National Natural Science Foundation of China (81902258), the Beijing Natural Science Foundation (7192127) and the Non-profit Central Research Institute Fund of Chinese Academy of Medical Sciences (2019-RC-HL-006). Wei Ge was supported by the National Natural Science Foundation of China (81971023). Chen Li was supported by the CAMS Innovation Fund for Medical Sciences

(CIFMS) (2017-I2M-3-001). Yanyu Chen was supported by the Graduate innovation fund of Peking Union Medical College (2019-1001-04).

### ORCID iDs

Chen Li  <https://orcid.org/0000-0002-8527-1680>

Wei Ge  <https://orcid.org/0000-0002-9907-512X>

### Supplemental material

Supplemental material for this article is available online.

### References

1. Chamot AM, Benhamou CL, Kahn MF, *et al.* [Acne-pustulosis-hyperostosis-osteitis syndrome. Results of a national survey. 85 cases]. *Rev Rhum Mal Osteoartic* 1987; 54: 187–196.
2. Rukavina I. SAPHO syndrome: a review. *J Child Orthop* 2015; 9: 19–27.
3. Li C, Zuo Y, Wu N, *et al.* Synovitis, acne, pustulosis, hyperostosis and osteitis syndrome: a single centre study of a cohort of 164 patients. *Rheumatology (Oxford)* 2016; 55: 1023–1030.
4. Nguyen MT, Borchers A, Selmi C, *et al.* The SAPHO syndrome. *Semin Arthritis Rheum* 2012; 42: 254–265.
5. Liu S, Tang M, Cao Y, *et al.* Synovitis, acne, pustulosis, hyperostosis, and osteitis syndrome: review and update. *Ther Adv Musculoskelet Dis* 2020; 12: 1759720x20912865.
6. Assmann G and Simon P. The SAPHO syndrome—are microbes involved? *Best Pract Res Clin Rheumatol* 2011; 25: 423–434.
7. Del Castillo FJ, Caniego T, Hurtado-Nédélec M, *et al.* THU0466 unraveling the genetic basis of familial SAPHO syndrome with next-generation sequencing. *Ann Rheum Dis* 2014; 73: 344–344.
8. Hurtado-Nedelec M, Chollet-Martin S, Chapeton D, *et al.* Genetic susceptibility factors in a cohort of 38 patients with SAPHO syndrome: a study of *PSTPIP2*, *NOD2*, and *LPIN2* genes. *J Rheumatol* 2010; 37: 401–409.
9. Takayanagi H. Osteoimmunology and the effects of the immune system on bone. *Nat Rev Rheumatol* 2009; 5: 667–676.
10. Guder C, Gravius S, Burger C, *et al.* Osteoimmunology: a current update of the interplay between bone and the immune system. *Front Immunol* 2020; 11: 58.
11. Weitzmann MN and Oforokun I. Physiological and pathophysiological bone turnover—role of the immune system. *Nat Rev Endocrinol* 2016; 12: 518–532.
12. Charles JF and Aliprantis AO. Osteoclasts: more than ‘bone eaters’. *Trends Mol Med* 2014; 20: 449–459.
13. Vikulina T, Fan X, Yamaguchi M, *et al.* Alterations in the immuno-skeletal interface drive bone destruction in HIV-1 transgenic rats. *Proc Natl Acad Sci USA* 2010; 107: 13848–13853.
14. Xie Y, Chen Y, Zhang L, *et al.* The roles of bone-derived exosomes and exosomal microRNAs in regulating bone remodelling. *J Cell Mol Med* 2017; 21: 1033–1041.
15. Lyu H, Xiao Y, Guo Q, *et al.* The role of bone-derived exosomes in regulating skeletal metabolism and extraosseous diseases. *Front Cell Dev Biol* 2020; 8: 89.
16. Buzas EI, György B, Nagy G, *et al.* Emerging role of extracellular vesicles in inflammatory diseases. *Nat Rev Rheumatol* 2014; 10: 356–364.
17. Ekström K, Omar O, Granéli C, *et al.* Monocyte exosomes stimulate the osteogenic gene expression of mesenchymal stem cells. *PLoS One* 2013; 8: e75227.
18. Man QW, Zhang LZ, Zhao Y, *et al.* Lymphocyte-derived microparticles stimulate osteoclastogenesis by inducing RANKL in fibroblasts of odontogenic keratocysts. *Oncol Rep* 2018; 40: 3335–3345.
19. Pieters BCH, Cappariello A, Van Den Bosch MHJ, *et al.* Macrophage-derived extracellular vesicles as carriers of alarmins and their potential involvement in bone homeostasis. *Front Immunol* 2019; 10: 1901.
20. Cao Y, Li C, Xu W, *et al.* Spinal and sacroiliac involvement in SAPHO syndrome: a single center study of a cohort of 354 patients. *Semin Arthritis Rheum* 2019; 48: 990–996.
21. Chen Y, Xie Y, Xu L, *et al.* Protein content and functional characteristics of serum-purified exosomes from patients with colorectal cancer revealed by quantitative proteomics. *Int J Cancer* 2017; 140: 900–913.
22. Kim J, Yang J, Park OJ, *et al.* Serum amyloid A inhibits osteoclast differentiation to maintain macrophage function. *J Leukoc Biol* 2016; 99: 595–603.

23. Oh E, Lee HY, Kim HJ, *et al.* Serum amyloid A inhibits RANKL-induced osteoclast formation. *Exp Mol Med* 2015; 47: e194.
24. Kim KW, Kim BM, Moon HW, *et al.* Role of C-reactive protein in osteoclastogenesis in rheumatoid arthritis. *Arthritis Res Ther* 2015; 17: 41.
25. Nishida M, Saegusa J, Tanaka S, *et al.* S100A12 facilitates osteoclast differentiation from human monocytes. *PLoS One* 2018; 13: e0204140.
26. Wang X, Wei W, Krzeszinski JY, *et al.* A liver-bone endocrine relay by IGFBP1 promotes osteoclastogenesis and mediates FGF21-induced bone resorption. *Cell Metab* 2015; 22: 811–824.
27. Li S, Liu B, Zhang L, *et al.* Amyloid beta peptide is elevated in osteoporotic bone tissues and enhances osteoclast function. *Bone* 2014; 61: 164–175.
28. Bi Y, Nielsen KL, Kilts TM, *et al.* Biglycan deficiency increases osteoclast differentiation and activity due to defective osteoblasts. *Bone* 2006; 38: 778–786.
29. Parisuthiman D, Mochida Y, Duarte WR, *et al.* Biglycan modulates osteoblast differentiation and matrix mineralization. *J Bone Miner Res* 2005; 20: 1878–1886.
30. Ikegawa S. Expression, regulation and function of asporin, a susceptibility gene in common bone and joint diseases. *Curr Med Chem* 2008; 15: 724–728.
31. Ueda M, Goto T, Kuroishi KN, *et al.* Asporin in compressed periodontal ligament cells inhibits bone formation. *Arch Oral Biol* 2016; 62: 86–92.
32. Nakamura YS, Hakeda Y, Takakura N, *et al.* Tyro 3 receptor tyrosine kinase and its ligand, Gas6, stimulate the function of osteoclasts. *Stem Cells* 1998; 16: 229–238.
33. Yamoah K, Brebene A, Baliram R, *et al.* High-mobility group box proteins modulate tumor necrosis factor- $\alpha$  expression in osteoclastogenesis via a novel deoxyribonucleic acid sequence. *Mol Endocrinol* 2008; 22: 1141–1153.
34. Kim J-M, Lee K, Kim MY, *et al.* Suppressive effect of syndecan ectodomains and N-desulfated heparins on osteoclastogenesis via direct binding to macrophage-colony stimulating factor. *Cell Death Dis* 2018; 9: 1119.
35. Li X, Pennisi A and Yaccoby S. Role of decorin in the antimyeloma effects of osteoblasts. *Blood* 2008; 112: 159–168.
36. Horton JE, Harper J and Harper E. Platelet factor 4 regulates osteoclastic bone resorption in vitro. *Biochim Biophys Acta* 1980; 630: 459–462.
37. Chellaiah MA, Kizer N, Biswas R, *et al.* Osteopontin deficiency produces osteoclast dysfunction due to reduced CD44 surface expression. *Mol Biol Cell* 2003; 14: 173–189.
38. Reinholt FP, Hulthenby K, Oldberg A, *et al.* Osteopontin—a possible anchor of osteoclasts to bone. *Proc Natl Acad Sci USA* 1990; 87: 4473–4475.
39. Tian H, Bi X, Li C-S, *et al.* Secreted phosphoprotein 24 kD (Spp24) and Spp14 affect TGF- $\beta$  induced bone formation differently. *PLoS One* 2013; 8: e72645–e72645.
40. Yoshida K, Akita N, Okamoto T, *et al.* Activated protein C suppresses osteoclast differentiation via endothelial protein C receptor, protease-activated receptor-1, sphingosine 1-phosphate receptor, and apolipoprotein E receptor 2. *Thromb Res* 2018; 163: 30–40.
41. Szweras M, Liu D, Partridge EA, *et al.*  $\alpha$ 2-HS glycoprotein/fetuin, a transforming growth factor- $\beta$ /bone morphogenetic protein antagonist, regulates postnatal bone growth and remodeling. *J Biol Chem* 2002; 277: 19991–19997.
42. Colina M, Govoni M, Orzincolo C, *et al.* Clinical and radiologic evolution of synovitis, acne, pustulosis, hyperostosis, and osteitis syndrome: a single center study of a cohort of 71 subjects. *Arthritis Rheum* 2009; 61: 813–821.
43. Hayem G, Bouchaud-Chabot A, Benali K, *et al.* SAPHO syndrome: a long-term follow-up study of 120 cases. *Semin Arthritis Rheum* 1999; 29: 159–171.
44. Przepiera-Będzak H, Fischer K and Brzosko M. Serum levels of angiogenic cytokines in psoriatic arthritis and SAPHO syndrome. *Pol Arch Med Wewn* 2013; 123: 297–302.
45. Gabay C and Kushner I. Acute-phase proteins and other systemic responses to inflammation. *N Engl J Med* 1999; 340: 448–454.
46. Zhang Y, Zhang J, Sheng H, *et al.* Acute phase reactant serum amyloid A in inflammation and other diseases. *Adv Clin Chem* 2019; 90: 25–80.
47. Nys G, Cobraiville G, Servais AC, *et al.* Targeted proteomics reveals serum amyloid A variants and alarmins S100A8-S100A9 as key plasma biomarkers of rheumatoid arthritis. *Talanta* 2019; 204: 507–517.
48. Huang Y, Feng F, Huang Q, *et al.* Proteomic analysis of serum-derived extracellular vesicles in ankylosing spondylitis patients. *Int Immunopharmacol* 2020; 87: 106773.



49. Liu S, Ji W, Lu J, *et al.* Discovery of potential serum protein biomarkers in ankylosing spondylitis using tandem mass tag-based quantitative proteomics. *J Proteome Res* 2020; 19: 864–872.
50. Wekell P, Björnsdóttir H, Björkman L, *et al.* Neutrophils from patients with SAPHO syndrome show no signs of aberrant NADPH oxidase-dependent production of intracellular reactive oxygen species. *Rheumatology (Oxford)* 2016; 55: 1489–1498.
51. Fremerey J, Morozov P, Meyer C, *et al.* Nucleolin controls ribosome biogenesis through its RNA-binding properties. *Blood* 2016; 128: 5056–5056.
52. Durut N and Sáez-Vásquez J. Nucleolin: dual roles in rDNA chromatin transcription. *Gene* 2015; 556: 7–12.
53. Ginisty H, Amalric F and Bouvet P. Nucleolin functions in the first step of ribosomal RNA processing. *EMBO J* 1998; 17: 1476–1486.
54. Roger B, Moisan A, Amalric F, *et al.* Nucleolin provides a link between RNA polymerase I transcription and pre-ribosome assembly. *Chromosoma* 2003; 111: 399–407.
55. Lemma S, Sboarina M, Porporato PE, *et al.* Energy metabolism in osteoclast formation and activity. *Int J Biochem Cell Biol* 2016; 79: 168–180.
56. Kubatzky KF, Uhle F and Eigenbrod T. From macrophage to osteoclast—how metabolism determines function and activity. *Cytokine* 2018; 112: 102–115.
57. Xie Y, Gao Y, Zhang L, *et al.* Involvement of serum-derived exosomes of elderly patients with bone loss in failure of bone remodeling via alteration of exosomal bone-related proteins. *Aging Cell* 2018; 17: e12758–e12758.
58. Robbins PD and Morelli AE. Regulation of immune responses by extracellular vesicles. *Nat Rev Immunol* 2014; 14: 195–208.
59. Kim SH, Bianco NR, Shufesky WJ, *et al.* MHC class II+ exosomes in plasma suppress inflammation in an antigen-specific and Fas ligand/Fas-dependent manner. *J Immunol* 2007; 179: 2235–2241.
60. Firinu D, Barca MP, Lorrai MM, *et al.* TH17 cells are increased in the peripheral blood of patients with SAPHO syndrome. *Autoimmunity* 2014; 47: 389–394.
61. Jurewicz MM and Stern LJ. Class II MHC antigen processing in immune tolerance and inflammation. *Immunogenetics* 2019; 71: 171–187.
62. Grosjean C, Hurtado-Nedelec M, Nicaise-Roland P, *et al.* Prevalence of autoantibodies in SAPHO syndrome: a single-center study of 90 patients. *J Rheumatol* 2010; 37: 639–643.
63. Buchwald ZS, Kiesel JR, DiPaolo R, *et al.* Osteoclast activated FoxP3+ CD8+ T-cells suppress bone resorption in vitro. *PLoS One* 2012; 7: e38199.
64. Li HY, Hong SY, Qian JF, *et al.* Cross talk between the bone and immune systems: osteoclasts function as antigen-presenting cells and activate CD4+ and CD8+ T cells. *Blood* 2010; 116: 210–217.
65. Benasciutti E, Mariani E, Oliva L, *et al.* MHC class II transactivator is an in vivo regulator of osteoclast differentiation and bone homeostasis co-opted from adaptive immunity. *J Bone Miner Res* 2014; 29: 290–303.

Visit SAGE journals online  
journals.sagepub.com/  
home/tab

 SAGE journals